

Review

Cement-Free Binders in Alumina-Magnesia Refractory Castables— A Review

Luyan Sun^{1,2}, Donghai Ding^{1,*}, Guoqing Xiao^{1,3,*}, Jianjun Chen⁴ and Yuan Feng¹

¹ College of Materials Science and Engineering, Xi'an University of Architecture and Technology, Xi'an 710055, China; sunluyan2007@126.com (L.S.); fengyuan@xauat.edu.cn (Y.F.)

² Department of Architecture Engineering, Sichuan Polytechnic University, Deyang 618000, China

³ State Key Laboratory of Green Building in Western China, Xi'an University of Architecture and Technology, Xi'an 710055, China

⁴ College of Materials Science and Engineering, Luoyang Institute of Science and Technology, Luoyang 471000, China; c_jianjun@foxmail.com (J.C.)

* Corresponding author. E-mail: dingdongxauat@163.com (D.D.); xiaoguoqing@xauat.edu.cn (G.X.)

Received: 9 December 2024; Accepted: 13 February 2025; Available online: 21 February 2025

ABSTRACT: To solve the problem of the accelerated deterioration of calcium aluminate (CAC)-bonded alumina-magnesia refractory castables during the secondary refining process, the development of cement-free binders has emerged as one significant research field of castables. The hydration behavior, curing mechanism, and properties of the most recent research on cement-free binders are compared in this paper. The problems and the modification of each binder of recent research are summarized. High-temperature performance of the castables bonded by traditional hydraulic cement-free binders (ρ - Al_2O_3 and activated MgO) is outstanding, explosive spalling resistance of the castables bonded by sol binders (silica sol, alumina sol) is good, and the properties of the castables bonded by novel organic hydratable binder (hydratable magnesium citrate) combine the advantages of these two binders above, but the mid-temperature mechanical strength is low. Furthermore, alumina-magnesia castables bonded by organic-composited inorganic cement-free binders are expected to be a future domain.

Keywords: Cement-free binder; Refractory castables; Hydration process; Gas permeability; High-temperature performance



© 2025 The authors. This is an open access article under the Creative Commons Attribution 4.0 International License (<https://creativecommons.org/licenses/by/4.0/>).

1. Introduction

Alumina-magnesia refractory castables possess excellent high-temperature mechanical properties and corrosion resistance. They are mainly employed as the working layer of the ladle lining for steel production. Additionally, they can also be utilized for the overall lining of ladle permeable plugs, argon-blowing lances, or powder spraying lances, et al. [1,2]. The alumina-magnesia castables are made by mixing continuously graded Al_2O_3 aggregate (such as fused white corundum, tabular corundum, or fused high alumina corundum), Al_2O_3 fine powder, MgO fine powder, or magnesia-alumina spinel powder, modified fine powder, additives, and binders with water, followed by casting and molding. The microstructure of the castables is illustrated in Figure 1 [2]. The in-situ magnesia-alumina spinel formed by the reaction between Al_2O_3 and MgO components enhanced the slag corrosion resistance of the castables, which are mainly used in ladle sidewalls and impact pads to resist slag infiltration, corrosion, and local thermal shock [3]. However, it is necessary to control the MgO content in the range of 6–8 wt.% to prevent excessive linear expansion. The castables with the direct addition of magnesia-alumina spinel powder with the content of 10–20 wt.% are suitably applied in the bottom of the ladle due to the good volume stability and high strength [4]. It is utilized to withstand the impact of pouring liquid steel and to bear the load of steel and slag.

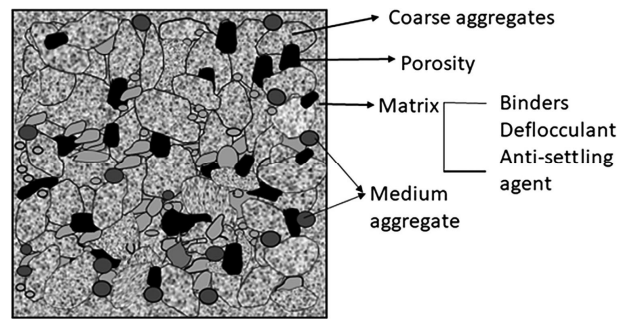


Figure 1. Microstructure of refractory castables [1]. Reprinted with permission from Ref. [1] Copyright 2014, Wiley.

The binders with different physicochemical properties and bonding methods are intricately associated with the service performance of the castables [5,6]. Calcium aluminate cement (CAC) is presently the most prevalent for alumina-magnesia refractory castables, which exhibited high strength, outstanding workability, chemical erosion and corrosion resistance. However, low melting point phases such as anorthite ($\text{CaAl}_2\text{Si}_2\text{O}_8$) and gehlenite ($\text{Ca}_2\text{Al}_2\text{SiO}_7$) can be easily generated due to the reaction between CaO contained in CAC, and SiO_2 and Al_2O_3 in the castables, and the high-temperature properties of the refractory castables are reduced, which limits the application of the CAC bonded castables under the harsh environmental conditions of modern extra-furnace refining [7,8]. In addition, a large amount of crystalline water is contained in hydration products like CAH_{10} and C_2AH_8 , and during heat treatment, the dehydration of these hydration products will lead to a decrease in the mechanical strength of the castables and an increase in the risk of explosive spalling of the castables.

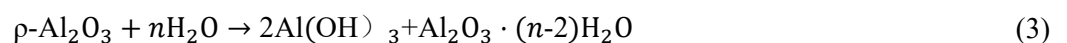
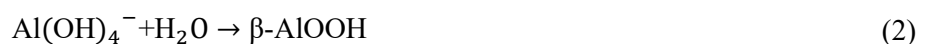
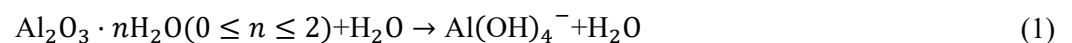
The improvement of the high-temperature service performance and explosive spalling resistance of CAC-bonded castables can be achieved by reducing the cement content and modulating the hydration process and the hydration product composition. Traditional CAC-bonded castables ($\text{CaO} > 2.5 \text{ wt.}\%$) were developed into low cement castables [9] (LCCs, $1.0 \text{ wt.}\% < \text{CaO} < 2.5 \text{ wt.}\%$) and ultra-low cement castables [5,10] (ULCCs, $0.2 \text{ wt.}\% < \text{CaO} < 1.0 \text{ wt.}\%$), and certain amounts of micro and ultra-micro powders such as micro SiO_2 and activated Al_2O_3 , need to be added to enhance the mechanical strength of the castables [11]. Therefore, the development of cement-free binder systems and the transformation of the bonding mode of the castables from hydrated to cohesive bonding are effective means by which the high-temperature performance of alumina-magnesia castables can be enhanced and the risk of explosive spalling can be reduced [12,13].

2. Traditional Hydraulic Binding Cement-Free Binders

2.1. $\rho\text{-Al}_2\text{O}_3$

2.1.1. Hydration Behavior and the Problems

$\rho\text{-Al}_2\text{O}_3$ (HA) is the product of alumina trihydrate after rapid calcination at 600–900 °C. There are no impurity components in HA, and the generation of low melting point phases in the castables can be avoided, so that good slag corrosion resistance and creep resistance can be possessed by the castables [14]. The castables bonded by HA binders are similar with respect to the hardening mechanism to LCCs and ULCCs. HA binder is of high activity, a lamellar structure, and a high specific surface area (100–200 m^2/g) [15,16]. In the hydration process of HA, HA particles are dissolved in water and $\text{Al}(\text{OH})_4^-$ ions are released (reaction Equation (1)) [17]. After reaching the saturated concentration, an amorphous layer of pseudo-bohmite gel is precipitated (reaction Equation (2)), and a small portion of them is converted into boehmite gel ($\text{Al}_2\text{O}_3(1-2)\text{H}_2\text{O}$), and a majority of them are converted into bayerite crystals ($\text{Al}_2\text{O}_3 \cdot 3\text{H}_2\text{O}$) (reaction Equation (3)) [6,18].



However, some drawbacks of HA binders exist: (1) A higher demand of water and a longer mixing time is required of the castables due to the large specific surface area of HA [19]; (2) The air pores are blocked by the proposed boehmite gel, resulting in the poor gas permeability of the hydration product, and the decomposition temperatures of the HA

hydration products in a narrow temperature range of 100–500 °C as shown in Table 1 investigated by Fábio et al., which led to a large risk of explosive spalling of the castables [20]. (3) The mechanical properties of the castables in the range of 300–1000 °C heat treatment are poor [21–23].

Table 1. Decomposition temperatures of the HA hydration products [20]. Reprinted with permission from Ref. [20]. Copyright 2004, Elsevier.

ρ -Al ₂ O ₃	Decomposition Temperature (°C)
Free-water release	From room temperature to 100 °C
Alumina gel and the boehmite decomposition	100–300
Bayerite decomposition	300–500

2.1.2. Modification

Thereby, the workability, mechanical properties and explosive spalling resistance of the castables are improved by regulating their hydration behavior and hydration products of the HA binder. Those are close to the factors including the HA particle size, pore surface properties, and additives [24,25]. Compared to large-sized particles (with a D50 of 20–50 µm), a continuous layer of thin sheet boehmite is more likely to be formed by small-sized HA particles (D50 of 10 µm). The green mechanical strength of the castables benefited from this, yet the water demand of the castables is caused to rise and the setting time is made to shorten [23]. Li et al. [16] found that the flow value increased from 173 mm to 206 mm and the hardening time is prolonged for the HA bonded castables by the HA binder particles being ball milled for 6 h, reducing the specific surface area of pores from 306.64 m²/g to 284.49 m²/g. And the specific surface area of pores of the HA particles can be further reduced to 177.53 m²/g through adding the magnesite powder (Mg₅(CO₃)₄(OH)₂·5H₂O) during the ball milling process [26]. This is because the magnesite powder, which has a similar lamellar structure, is inserted into lamellar ρ -Al₂O₃ particles and fills in the pores and cracks. However, the mechanical strength of the castables after drying is reduced by the above methods. The formation of the hydrate phases can be delayed by the additives. The dispersion of the particles in water can be improved by additives such as citric acid, and citrate by adsorbing on the surface of HA particles [27]. The addition of SiO₂ micropowder also can be distributed on the surface of the HA particles by the formation of SiO₂-AlOOH gel [28]. The hydration process of HA is effectively prevented from proceeding by all of these measures, resulting in extending the working time and affecting the density and strength of the castables. However, the high-temperature service performance of the castables can be reduced by SiO₂ micropowder.

The gas permeability of the bonded castables is improved by the increase in pore volume and large-size pores of the hydration products, but their mechanical strength and high-temperature properties are worse. The method for enhancing the gas permeability of HA-bonded castables is analogous to that of CAC-bonded castables. Organic fibers with a melting point HA of 150–200 °C can be effectively added so that the dehydration of Al(OH)₃ can be enabled to be quickly discharged, and the explosive spalling of the castables is likely to occur at 400 °C can be reduced and its resistance to thermal shock cannot be diminished [29]. Additionally, the explosive spalling resistance of the castables is effectively improved by the addition of H₂O₂ resulting in the increased average pore size of the pores in the castables. However, it has led to a reduction in bulk density and mechanical strength, and its content should be controlled at around 0.075 wt.% [30]. The gas permeability properties of CAC and HA bonded castables after the addition of different drying agents and SiO₂ sols are summarized in Figure 2: The gas permeability of the castables can be enhanced by the active compounds within the range of 80–150 °C, while the different fibers need to be within the range of 150–450 °C to be effective [31–36]. The gas permeability of CAC bonded castables can be most prominently enhanced by the fibers, whereas the gas permeability of HA castables is more beneficially improved by the active compounds. The gas permeability coefficients k_1 of CAC, HA and SiO₂ sol-bonded castables are shown in Figure 3 [31–37]. Among them, the best gas permeability is possessed by SiO₂ sol bonded castables with the coefficients in the range of 6–10 × 10⁻¹² m², nearly two or four orders of magnitude more than those of the CAC bonded castables after drying at 110 °C. The gas permeability of CAC bonded castables ranked second, with the coefficients in the range of 2–200 × 10⁻¹⁶ m² after drying at 110 °C. The worst one is of HA-bonded castables with a coefficient of 9 × 10⁻¹⁹ m², nearly three orders of magnitude lower than that of the CAC bonded castables after drying at 110 °C.

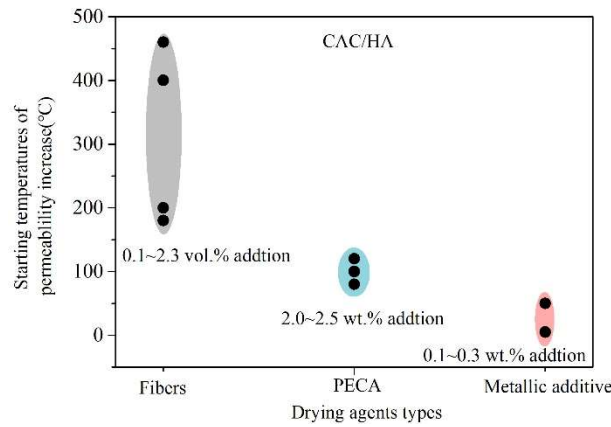


Figure 2. Starting temperature for enhancing the gas permeability for CAC and HA bonded castables by different drying agents [31–36]. Reprinted with permission from Ref. [31,32] Copyright 2004, Elsevier; [33,34] Copyright 2003, American Ceramic Society; [35] Copyright 2016, ECREF; [36] Copyright 2010, MRS.

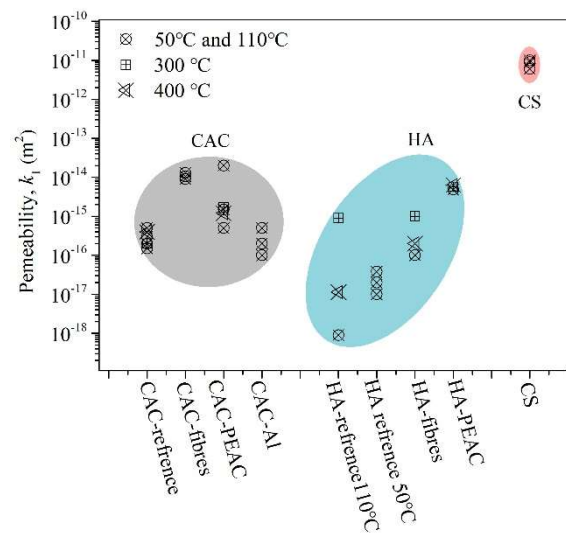


Figure 3. Effects of different drying agents and CS on the gas permeability coefficient k_1 of CAC and HA bonded castables [31–37]. Reprinted with permission from Ref. [31,32] Copyright 2004, Elsevier; [33,34] Copyright 2003, American Ceramic Society; [35] Copyright 2016, ECREF; [36] Copyright 2010, MRS; [37] Copyright 2018, ResearchGate.

2.2. Activated MgO

2.2.1. Hydration Behavior and the Problems

Similar to the HA binder, the activated MgO binder generated the bonding strength via hydration [38–40]. Moreover, it is introduced as a premium raw material into the high alumina-magnesia refractory castables. Additionally, Mn^{2+} , Fe^{2+} , and Fe^{3+} ions within the slag are liable to be captured by in-situ magnesia-alumina spinel for the formation of a solid solution, which effectively improved the slag corrosion resistance of the castables [41,42].

It is suggested by the current results that two hydration mechanisms of the activated MgO exist. One is the shrinkage nucleus mechanism proposed by Kitamura et al. [43], which is applicable to 135–200 °C. The other is the dissolution precipitation mechanism [44] researched by Rocha et al., which is applicable to 35–90 °C. The MgO particles are dissolved in water and the hydration reaction occurs on the surface of the particles to generate $MgOH^+$ ions. After reaching a saturated concentration with the OH^- ions in water, $Mg(OH)_2$ is made to begin to nucleate and grow up, and ultimately precipitate and deposit on the surface of the MgO particles.

The activated MgO binder reacts with water to form $Mg(OH)_2$, which has an expansion of 2.5 times its volume and leads to cracking of the castables during the curing process [45]. In addition, the dehydration of $Mg(OH)_2$ is concentrated in the range of 380–450 °C [46,47], and even reaches 500 °C under increased pressure, which is easy to cause the explosive spalling of the castables in the drying process, and a strict drying system is necessary to be developed.

2.2.2. Modification

The hydration process of activated MgO is affected by the type, size, and purity of MgO particles [48,49], the pH value, temperature, and admixtures. Based on the hydration kinetics of MgO, the cracking of the castables can be reduced by the control of the hydration process of MgO, and the commonly used measures are as follows:

Cracking is controlled by adding surfactants to accelerate the production of Mg(OH)₂ [50,51]. Commonly used surfactants [52,53] are mainly salts (ammonium chloride, magnesium acetate, magnesium nitrate and sodium acetate) and weak acids (nitric acid, acetic acid). When dissolved in water, anions are released by these additives and can be respectively adsorbed on O²⁻ or Mg²⁺. The nucleation site barriers of Mg(OH)₂ are lowered and the nucleation rate is increased. The crystal morphology of Mg(OH)₂ is also changed by formic, acetic and propionic acids [47,48], with the particles being made pliable and the compatibility with the pores of the castables being enhanced resulting in the reduction of the cracks [54].

The control of cracking was also achieved by delaying the generation of Mg(OH)₂ through the addition of additives such as inorganic salts [55,56] and citric acid [57]. Citric acid is currently a more effective retarder. The generation of Mg(OH)₂ is inhibited by the formation of a complex chelate on the surface of MgO particles resulting from the reaction between citrate ions and Mg²⁺. Chen et al. [58]. investigated the functional mechanism of citric acid on MgO hydration based on molecular dynamics. The adsorption energy of citric acid (−2.89 eV) adsorbed on the defective MgO (001) surface is more negative than that of H₂O (−2.49 eV), indicating that citric acid instead of the H₂O would easily bond with unsaturated Mg²⁺ at defects and defective MgO surfaces from hydration.

The SiO₂ micropowders are most commonly used in combination with activated MgO binders. As shown in Figure 4 [59], in alkaline aqueous solutions, HSiO₃⁻ ions can be ionized by SiO₂ and then adsorbed on the surface of MgO. Volume-stable hydrated magnesium silicate (M-S-H) can be generated [60–62], which can be produced in alkaline environments. M-S-H can be rapidly generated with the M/S of 0.9–1.1 and at temperatures of 50–70 °C [59,63]. Cracking in the casting can be controlled by directly adding pre-synthesized M-S-H. In the research [64,65], the formation of Mg(OH)₂ is effectively reduced by partial or total substitution of the reacted MgO binder. The dehydration products of M-S-H are divided into three stages: free water evaporation at 100–200 °C; Mg(OH)₂ decomposition at 400–600 °C; and M-S-H decomposition and formation of magnesium olivine at 600–800 °C. Compared with Mg(OH)₂, the range of dehydration temperature is wider and water vapour is lower than the dehydration products of M-S-H, by which the explosive spalling resistance of the castables is improved. However, when the specimen size is large, the addition of SiO₂ greater than 6.0 wt.% [66,67] is required to ensure that the specimen does not crack. It has also been noted that the decomposition temperature of the hydration products is increased and the flowability and gas permeability of the castables deteriorated with SiO₂ addition greater than 1.0 wt.%. While, the high-temperature mechanical strength and slag corrosion resistance of the castables will be reduced by excessive SiO₂ micropowder. The synthesis of M-S-H requires strict control of the MgO/SiO₂ molar ratio and pH, and the synthesis of hydrotalcite takes months to complete, causing the difficulty of large-scale production.

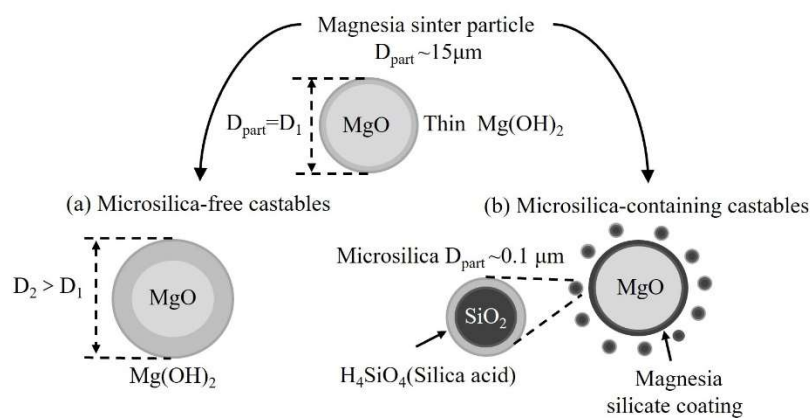


Figure 4. Schematic of the mechanism of the inhibiting activated magnesia hydration by micro silica [59]. Reprinted with permission from Ref. [59] Copyright 2014, Wiley.

The SiOX-Mag as an additive was developed by Santos Jr. et al. [68] and was applied to alumina-magnesia refractory castables, and superior explosive spalling resistance of the castables was shown compared to that with the addition of 1.0 wt.% SiO₂ micropowder. However, the permeable path formation and the mechanism of microstructure

improvement remain unclear. The SiO₂ micropowder with a content of 3.0–8.0 wt.% and an appropriate amount of SiO_xX-Mag were added to the activated MgO bonded castables reported by Hong [69] et al., and large test pieces without cracks were produced. If industrial scale application is to be achieved, a larger proportion of SiO₂ micropowder needs to be added. However, it is easy for SiO₂ to react with the oxides and impurities (CaO, FeO, and Al₂O₃, etc.) in the castables system, resulting in the formation of low melting point phases resulting in the deterioration of the high-temperature performance of the castables. The slurry made of MgO and SiO₂ micropowders, which were added to the castables by the wet milling process [70], can accelerate the formation of M-S-H and reduce the addition of SiO₂ micropowders. Consequently, the explosive spalling resistance of the castables can be significantly improved. Especially when 2.0–4.0 wt.% of SiO₂ micropowders are added, the cold modulus of rupture and the hot modulus of rupture of the castables are increased, respectively by 136.0% and 36.0%, and the thermal shock resistance is also significantly enhanced. M-S-H binder was prepared by the hydrothermal synthesis method using Na₂SiO₃·9H₂O and MgCl₂·6H₂O as raw materials by Zhang Yu et al. [62]. It was added to magnesium refractory castables for tundish lining, while the 3.0–6.0 wt.% SiO₂ micropowder needed to be added so that good mechanical strength and explosive spalling resistance at medium temperature could be achieved for the castables. The pre-synthesized M-S-H after firing at 200–400 °C was used as a binder for the castables by Li et al. [64], and the addition of SiO₂ micropowder was reduced to 1.0 wt.%. However, the synthesis process of M-S-H was cumbersome and the price was high.

The chelating agents are also used to improve the gas permeability of reactive MgO-bonded castables. Aluminum lactate (aluminum salt of 2-hydroxypropionic acid) [71] is used as a chelating agent for Mg²⁺ so that the generation of hydroxalite-like (Mg_xAl_y(OH)_{2x+2y}·y/2nH₂O) can be induced. The cracking of the castables is reduced and the explosive spalling resistance of the castables is enhanced [72], yet the green mechanical strength is decreased. Among the commonly used MgO raw materials (dead-burned magnesia sand, caustic magnesia sand, and light MgO micropowder), better gas permeability is exhibited by light MgO micropowder-bonded castables [73]. After heat treatment at 110–450 °C, the permeability coefficients k_1 and k_2 of the castables containing 1.0 wt.% aluminum lactate salt are 2×10^{-13} m² and 2×10^{-9} m respectively, which is two orders of magnitude better than that of magnesia sand-bonded castables. These k_1 and k_2 are four orders of magnitude higher than those of the CAC- and HA-bonded castables. The effects of four types of drying agents, polymer fibers (PF), organic aluminum salts (OAS-aluminium lactate), SiO₂-based additives (SM) and reactive compounds (MP), on the gas permeability and explosive spalling resistance of MgO-bonded castables are compared [65]. Although the polymer fibers are melted at –104 °C, they need to be fully decomposed (>300 °C) to act as a gas permeability enhancer. The incorporation of 1.0 wt.% SM does not inhibit the explosive spalling of the castables, and the pores in the castables are filled with the amorphous hydration products generated by the reaction between SM and Mg(OH)₂, which leads to a decrease in gas permeability.

The flowability of the refractory castables was significantly improved with no cracks during drying by using a slurry of MgO and silane coupling agent-modified silica sol made as a binder [74]. A negatively charged protective layer was formed on the MgO particles by the modified SiO₂, and the agglomeration of MgO particles was prevented. In addition, as the hydration reaction of MgO proceeded, the dissolution of SiO₂ was accelerated by the increase in pH value in the solution, and finally, a protective layer of Mg₅Si₈O₂₀(OH)₂·8H₂O was generated on MgO particles. This protective layer was transformed into a dense magnesium olivine (Mg₂SiO₄) layer by sintering. The mechanical strength of the matrix was significantly enhanced, but this method has not yet been popularized for application. The ultrafine MgO powder was used as a binder for refractory castables by Luz et al. [48], and its hydration rate was adjusted by formic acid resulting in no cracks in the castables during drying. The cold modulus of rupture of MgO-bonded refractory castables was similar to that of CAC bonded castables curing at 50 °C for 24 h, but the strength decreased rapidly after drying, and the gas permeability of the castables was poor.

The formation of Mg-Al hydroxalite (Mg₆Al₂CO₃(OH) 16·4H₂O) is induced under certain curing conditions in the MgO-bonded castable system by the addition of alumina sol, nano-Al₂O₃ micropowder or ρ -Al₂O₃. The reduction of the mechanical strength at mid-temperature is effectively slowed down as a result [75,76]. In addition, the wide temperature range of its decomposition is described as follows [77]: (1) <100 °C: free or adsorbed water is removed; (2) 100–200 °C: interlayer structural water is eliminated; (3) 300–400 °C: crystal dehydroxylation and decarbonization are carried out. A porous structure is formed inside the castables, and the burst resistance is enhanced.

The effects of the above methods on the decomposition temperature of the hydration products of the active MgO binder are shown in Figure 5 [71,72,78], and the effects on the mid-temperature mechanical strength of the castables are shown in Figure 6 [74,75]. It can be seen that the explosive spalling resistance and mid-temperature strength of the castables are enhanced by the addition of SiO₂ micropowder/sol, nano-Al₂O₃ micropowder/sol, etc. The gas permeability of the castables is enhanced by chelate additives, while there is a decrease in the mechanical strength.

Therefore, a significant challenge remains to be confronted despite the outstanding potential for the development of MgO-bonded alumina-magnesia refractory castables. Although certain research results have been obtained regarding the inhibition of hydration cracking of MgO-bonded castables under laboratory conditions, the issue of hydration cracking in large-scale industrial applications is still severely prevalent.

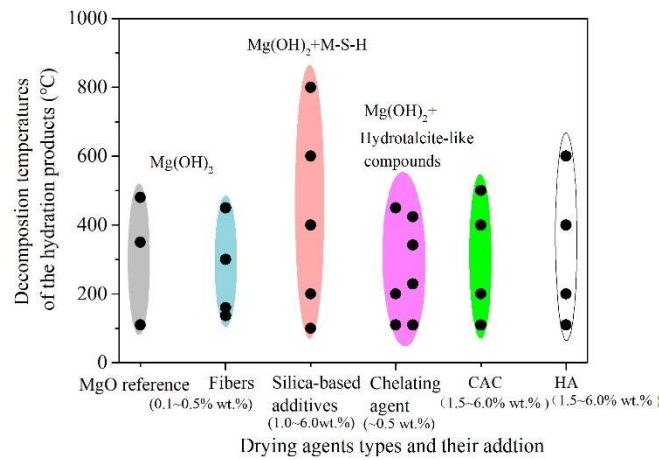


Figure 5. Decomposition temperatures of hydration products of activated MgO binder affected by the different additives and drying agents [71,72,78]. Reprinted with permission from Ref. [71] Copyright 2004, Elsevier; Ref. [72] Copyright 2015, ECREF, [78] Copyright 2010, Ceramic Society of Japan.

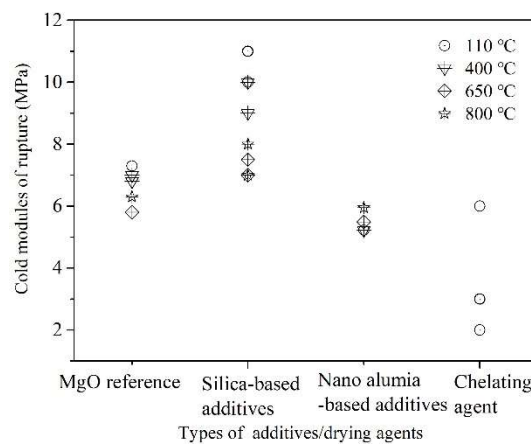


Figure 6. Cold modulus of rupture of activated MgO bonded refractory castables affected by the different additives and drying agents [74,75]. Reprinted with permission from Ref. [74,75] Copyright 2023, Elsevier.

3. Sol-Gel Binders

3.1. Silica Sol

3.1.1. Curing Mechanism and the Problems

Compared with traditional hydraulic binders, the sol-gel binders used for castables are suspensions of nanoparticles, and generated bonding strength by “gelling” or “flocculation” with no hydration products generated. The sol bonded castables have excellent explosive expelling resistance due to the permeable pore structure obtained after heat treatment [79]. As a type of sol-gel binder, silica sol (CS) was first utilized in practical production applications, good stability suspension, a solid content of 20–60 wt.%, a particle size of 8–80 nm, and high activity. The silanol groups (SiOH) and hydroxyl groups (-OH) are connected by collision reactions to create new bonds under different curing regimes [37], and “gelling” is achieved (Figure 7).

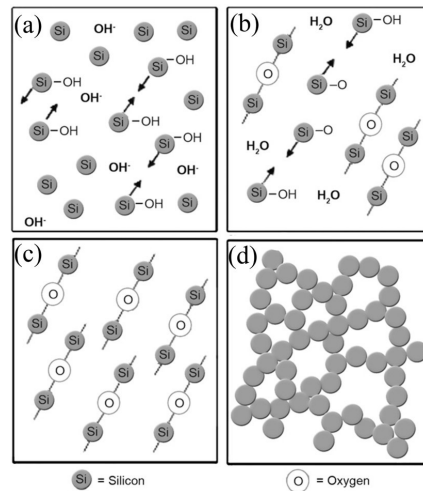


Figure 7. Colloidal silica gelling mechanism [51]: (a) silicon hydroxyl groups (Si-OH) covered on the surface of particles; (b) Dehydration between silicon hydroxyl groups; (c) Siloxane bonds (-Si-O-Si-) formation; (d) three-dimensional network of SiO₂ particles [37] Reprinted with permission from Ref. [51] Copyright 1999, Wiley; Ref. [37] Copyright 2018, ResearchGate.

A kinetic model of the SiO₂ sol gelation process was established by Wen et al. [80] for the verification of the gelling mechanism (Figure 8). Within the SiO₂ sol, a silica-oxygen network is formed. The polysilicon acid is created as a result of SiO₂ being dissolved in water. Si-O branched chains are produced through the polymerization of the ionized Si(OH)₃O⁻ with silanol present on the particle surface. The speed of gelling is determined by the growth rate of the Si-O branched chains. The acceleration of gelation can be attained by enhancing the ionization of silanol or decreasing the ionization rate of silicic acid.

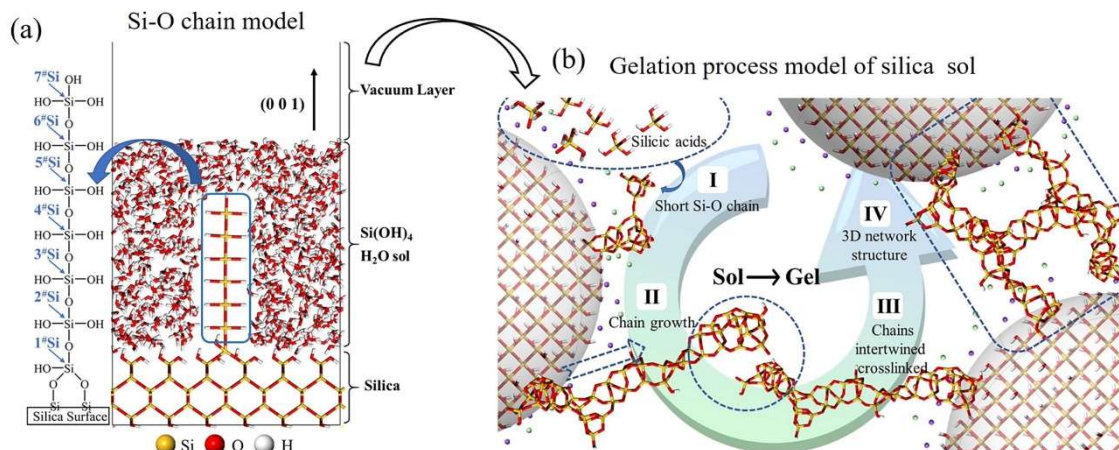


Figure 8. Molecular dynamics model of the gelation process of silica sol [80], the “#” in the figure represents the alcohol hydroxyl network “OH-Si-OH”. Reprinted with permission from Ref. [80] Copyright 2023, Elsevier.

However, CS utilized as a binder has the following drawbacks. Firstly, it is hard for the storage and transportation of the suspended liquid state of CS, and it is liable to solidify at low temperatures. Secondly, the generation of a liquid phase within the castables is contributed to by an excessive quantity of SiO₂, which leads to a reduction in the refractoriness of the refractory castables. As a result, its employment as a binder for ladle lining castables is limited, with the maximum operational temperature being restricted to 1600 °C [81,82].

3.1.2. Modification

The solidification of CS can be modulated through the alteration of pH, electrolyte concentration, temperature, as well as the particle size and concentration of SiO₂. It was discovered by Nouri-Khezrabad et al. [83,84] that the modulation of the pH value of CS from 3 to 5 leads to a more rapid solidification of CS. When the pH value is greater than 3.5, the addition of salts (e.g., NaCl) and organic liquids can be employed to induce the promotion of colloidal coagulation [83]. Additionally, the flocculation of gel particles can be actuated by the addition of curing agents like Al₂O₃, MgO, SiO₂, CaO, Mg(OH)₂, MgCl₂, and CaCl₂ [84]. Simultaneously, excellent operational characteristics can be bestowed upon the castables. Taking MgO as an example, when it is incorporated into CS, Mg(OH)₂ is generated.

This substance is capable of seizing H^+ from the Si-OH group, thereby expediting the formation of siloxane bonds (Figure 9). The gelation of CS can be instigated by both heat treatment [85] and freeze-drying [86]. A microporous structure (with gel pores $< 0.03 \mu\text{m}$) is acquired by the cured CS gel, which endows the castables with favorable gas permeability and facilitates the prompt repair of the castable lining under high-temperature circumstances.

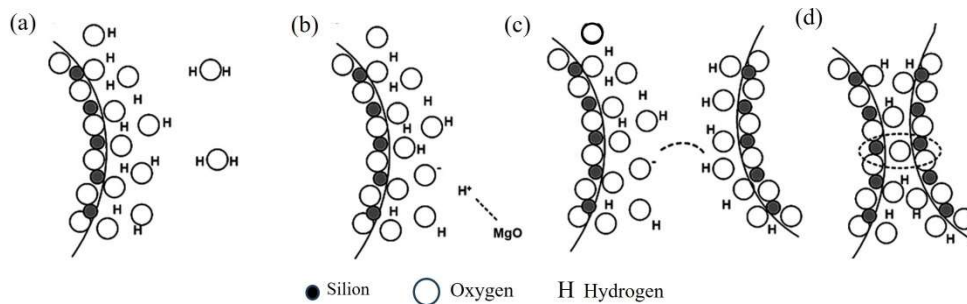


Figure 9. Schematic representation of colloidal silica consolidation promoted by MgO: (a) colloidal silica particle surface; (b) MgO addition; (c) siloxane bonds formation; (d) siloxane bonding ($-\text{Si}-\text{O}-\text{Si}-$) [15]. Reprinted with permission from Ref. [15] Copyright 2020, Springer.

In alumina-magnesia castable systems, the formation of mullite ($\text{Al}_6\text{Si}_2\text{O}_{13}$) is enabled by the reaction of nano- SiO_2 and Al_2O_3 at $1200 \text{ }^\circ\text{C}$ [87]. Thereby, the high-temperature mechanical properties of the castables are enhanced. Simultaneously, the surfaces of activated Al_2O_3 particles are adsorbed upon by the CS, the pores in the matrix are filled up, and sintering and matrix densification are spurred.

3.2. Alumina Sol

3.2.1. Alumina Sol Structure and Curing Mechanism

Consequently, to solve the drawback of silica sol, alumina sols (CA) were developed. Comparatively, the melting point of the alumina is much greater than that of silica. Also, the bulk density, strength, and other refractory/physical properties are quite superior to that of silica. There are mainly two methods used to synthesize alumina sols, including organic (alkoxides) and inorganic (salts) feedstock methods. Sarathchandran et al. reported an organic method to synthesize CA using nano boehmite ($\gamma\text{-AlOOH}$) with aluminum opropoxide serving as a precursor and a strong acid was added as a stabilizer [88]. On the other hand, the inorganic raw material method [89,90] was implemented by using HCl, nitric acid, or citric acid added to aluminum metal, aluminum salts, or Al_2O_3 powder. This CA was characterized by a low production cost yet a high impurity content and harmful gases emitted at elevated temperatures. A structural model [88] of the CA, as illustrated in Figure 10, was centered around a positively charged gel nucleus, with a bilayer structure consisting of adsorption and diffusion layers being formed.

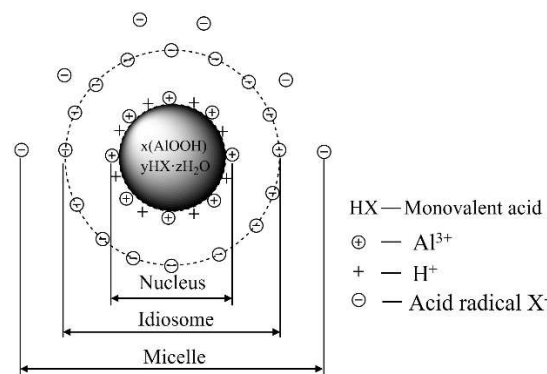


Figure 10. Aluminum sol structural model [88]. Reprinted with permission from Ref. [88] Copyright 2023, SZTE.

A molecular structure of the pseudo-boehmite (Figure 11) is configured with a coplanar-connected double-layered octahedral crystal structure [91]. Highly polarized and stable groups of aluminum hydroxyl ($\text{Al}-\text{OH}$) are situated on its surface. A larger quantity of oxygen vacancies gives rise to abundant positively charged active sites. The interlayer water is adsorbed onto the groups of $\text{Al}-\text{OH}$ via hydrogen bonding, a process that expands the space between the double-layered octahedra, thereby elongating the $\text{Al}-\text{O}$ bonds and shortening the $\text{Al}-\text{OH}$ bonds. Milani et al. reported that the

greater the amount of interlayer water, the more H^+ is absorbed by groups of the hydroxyl of pseudo-boehmite, and the more pronounced the gelling ability becomes [91]. The curing of CA bonded castables will occur by the physical and chemical mechanisms: the dehydration of the hydroxyl groups on the surface of the γ -AlOOH particles leads to the formation of Al-O-Al bonds and the gel formed by heat treatment [92].

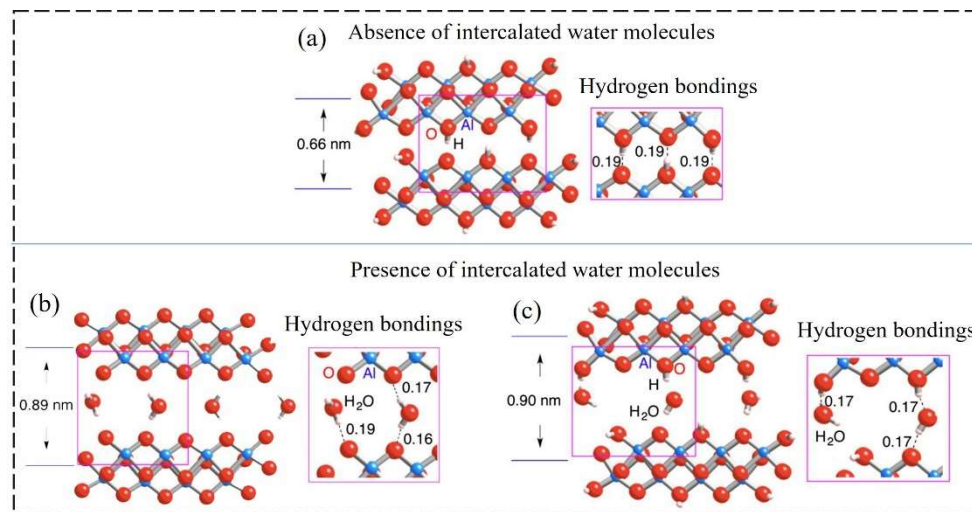


Figure 11. Crystal structure of one-dimensional nanowires of pseudo-boehmite: (a) absence of intercalated water; some terminated O atoms are bound (b) and not bound with H atoms (c) [90]. Reprinted with permission from Ref. [90] Copyright 2016, PNAS.

3.2.2. Problems and Modification

The application of pseudo-boehmite gel as a refractory binder has received relatively few reports. It is typically utilized in the production of functional ceramics as a binder, as an adsorbent for heavy metal ions, and in other research domains [93,94]. In comparison to that of CS, any low melting phase formation in the CA bonded castables, increases the high-temperature properties and corrosion resistance of the refractory. However, the green mechanical strength of castables cured at low temperatures is even lower than that of CS on account of the low solid content and weak bonding ability of CA. The industrial applications of the CA are limited due to low flowability, poor stability of sol, poor workability, and uncontrollable curing conditions, although it is a certain degree effective of induction of CA curing by the utilization of curing agents and additives [95].

The flowability of CA-bonded castables is suitable when the additions (in terms of solids) of CA are customarily regulated within the range of 1.0 to 4.0 wt.% [96]. The mechanical properties and slag corrosion resistance of the castables will be deteriorated with the addition exceeding 4% causing the water demand augmented. The curing of sols can also be affected either by pH alterations (Δ pH mechanism), by an increase in the strength of ionic solution (Δ I mechanism) [97,98], or by the additives of urea, formamide, and ammonium carbamate through transforming the ionic strength of the solution, thereby expediting the curing of CA. The gelation process was studied about the ionic concentration by the phase diagrams of the pseudo-boehmite gel suspensions. It was deduced that a higher ionic strength renders gelation more facile at low ionic concentrations, whereas a lower ionic strength facilitates gelation more readily at high ionic concentrations, by the variation in dynamic shear viscosity [99]. A method integrating both physical and chemical curing mechanisms was propounded by Grządka et al. [100], where alginate was employed as the gel precursor and hydroxy aluminum diacetate (HADA) as a retarder/accelerator. Alterations in the ionic concentration and pH within the sol were instigated by dissolution, giving rise to physical flocculation, and chemical gelling was actuated by the cross-linking of hydroxy-aluminum glycolic acid and aluminum ions with one another. Conversely, ammonium polyacrylate was utilized as a dispersing agent by Prabhakaran et al. [101] along with the addition of MgO. The flocculation of CA was precipitated by the Mg, because the Mg^{2+} ions were generated and adsorbed onto the nano- Al_2O_3 particles after MgO dissolved in water. Furthermore, the Mg^{2+} interacted with the dispersed polyacrylate ions in the solution to engender Mg-polyacrylic acid. However, the aforementioned curing agents are capable of promoting CA curing, further substantiation is requisite for industrial application.

The sol bonded castables can be subjected to high-temperature heat treatment without the prerequisite of initial drying at 100 °C resulting form no hydrated phase generation during the curing process and the formation of a porous structure during the gelation process of the castables. It was ascertained by Braulio et al. [83] that when refractory castables bonded with CS and CA were heated to 800 °C at a heating rate of 20 K/min, the weight loss of the castables

was merely approximately 0.25 wt.%, which is substantially lower than that of CAC-bonded castables (around 1.9 wt.%) and HA-bonded castables (around 0.6 wt.%). This concurs with the research of Ismael et al. [102], and it is inferred that CS and CA-bonded castables are endowed with a high level of gas permeability, even exceeding that of LCCs and ULCCs after the addition of polypropylene fibers, which markedly curtails the installation and maintenance times of the ladle liners. Nevertheless, the occurrence of drying cracks within the castables is prone to be induced with CS of high solid content and a particle size less than 14 nm.

Compared with hydraulic binders, within the temperature range from room temperature to 600 °C, a relatively lower mechanical strength is manifested by CS and CA bonded castables, which is enhanced by improving the curing temperature. It was investigated by Braulio et al. [96] that the mechanical strength of CA-bonded refractory castables with the CA addition of 4.0 wt.% cured at 50 °C is comparable to that of CAC-bonded castables. It's worth noting that there is a significant increase in mechanical strength of CS and CA bonded castables [103–105], attaining 5 MPa at 800 °C, and even reaching 8 MPa at 1000 °C of CS-bonded castables, which is twice the magnitude of that of CAC-bonded refractory castables, while a sharp decrease in mechanical strength of the CAC and HA bonded castables is exhibited after heat treatment of 600–1000 °C (Figure 12). It is shown that sintering was promoted by CS, and the high-temperature performance of the castables is further improved due to the formation of mullite. Thus, CS is more suitable as a refractory castable binder for aluminum smelting or for the kiln of the chemical industry with a service environment of low temperature. To induce the drawbacks of SiO₂ at low temperatures, a composite utilization of CS and CAC is used. The mechanical strength of the castables after drying is up to 4.29 MPa, 62–81% of the strength of CAC-bonded castables can be achieved even after heat treatment at 110–800 °C and 115–148% can be reached after heat treatment at 1100–1400 °C. Meanwhile, the target of fast drying at high temperature is also achieved [106]. Similarly, other novel sols such as mullite sols [107] and magnesia-alumina spinel sols [108,109] have been developed. Nevertheless, the sol binders remain in the laboratory research stage due to the challenges associated with the high cost during the process of production and preparation, and the low green mechanical strength of the castables.

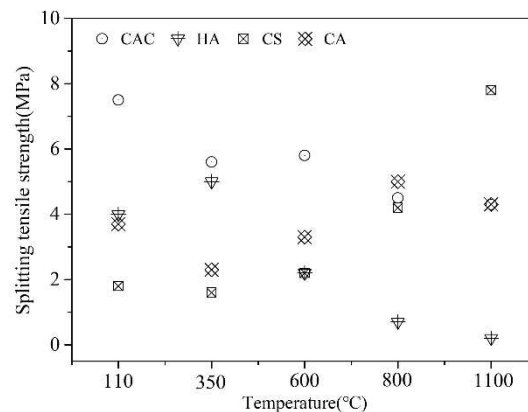


Figure 12. Splitting tensile strength as a function of heat treatment temperatures for CAC, HA, CS, and CA bonded castables [96,103]. Reprinted with permission from Ref. [96] Copyright 2011, ECREF; Ref. [103] Copyright 2006, Secar.

4. Organic Hydratable Magnesium Citrate Binder

4.1. Hydration Behavior and Problems

Based on the study of active MgO binder, hydratable magnesium citrate (HMC) was prepared by Chen et al. [110] by removing the water of crystallization from magnesium citrate hydrate. The HMC can be quickly dissolved and hydrated, highly crystalline magnesium citrate hydration products are generated, and a three-dimensional network structure is formed, so that a high green mechanical strength is presented by the castables. In the alumina-magnesia castable system, the additional amount of HMC binder is 3–5 wt.%. Excellent volume stability is exhibited of the castables in the curing and drying process, and the mechanical strength similar to that of the CAC bonded castables is obtained after heat treatment at 110 °C. The cold modulus of rupture after drying is 8–13 MPa, and it is 17–21 MPa after heat treatment at 1500 °C. The hydration product of magnesium citrate is an organic material, and nano-MgO (about 100 nm) was obtained after its decomposition during heat treatment, and micron magnesia-alumina spinel can be generated in situ by reacting with Al₂O₃ at 1100 °C. The thermal shock resistance and slag corrosion resistance of the castables are significantly improved [111]. The cold modulus of rupture of the castables after thermal shock after

three water-cooling cycles can be up to 5–6 MPa, which is 23–30% higher than that of CAC-bonded castables, and the slag corrosion resistance is better. Therefore, HMC is a very promising magnesia binder.

However, the mid-temperature mechanical strength of the castables was significantly decreased due to the decomposition of the hydration products of HMC. Especially, the mid-temperature mechanical strength at 500 °C was only 0.4–0.5 MPa.

4.2. Modification

Magnesium carboxylate borate ester as a new hydration product was formed by the reaction between boric acid and HMC with 1.0–1.5 wt.% boric acid added in the HMC bonded castables. The decomposition temperature of magnesium citrate-borate was increased by about 80 °C compared with that of the hydration products of HMC, by which the mid-temperature mechanical strength of the castables after 400 °C heat treatment was 12 times improved. However, the slag corrosion resistance was reduced [112]. In addition, the organization and properties of steel could be improved by a moderate amount of boron in the steel billet, but if the content was too large, the hardenability, strength and hardness of steel would be decreased [113]. Therefore, the use of boric acid needs to be coordinated with the steelmaking process and strictly controlled.

The activated nano-MgO was obtained by HMC after heat treatment at 1100 °C, which was added to the HMC-bound alumina-magnesia castable system containing a small amount of SiO₂ micropowder and the M-S-H generated. As a result, the mid-temperature mechanical strength of the castables after heat treatment at 800 °C was enhanced. However, the mid-temperature mechanical strength of the castables after heat treatment at 500–600 °C has not been investigated [114]. The thermal shock and slag corrosion resistance of the castables was significantly improved, attributed to the in-situ formation of magnesia-alumina spinel by the reaction of 1.5–2.0 wt.% of submicron Al₂O₃ with nano-MgO, but the mid-temperature mechanical strength of the castables heat treated at 500–800 °C was not improved.

In addition, the setting time is short and the flowability is poor of HMC bonded castables, resulting from the rapid hydration reaction of HMC, which failed to meet the construction requirements of the castables. The above performance of the castables could be improved by adding 0.01–0.02 wt.% of MgCl₂, but the mechanical strength of the castables was reduced. New hydration products could be generated by using SiO₂ gel to modify the HMC binder (HMC/silica sol binder), and the thermal stability of the hydration product was improved. The cold modulus of rupture of the castables after heat treatment at 500 °C was 267% improved compared with the HMC-bonded castables [115]. Moreover, the gas permeability of the castables could be enhanced by the microporous structure of the silica gel. The SiO₂ content should be controlled at 1.0–1.5 wt.%. However, due to the decomposition of organic hydration products, the mechanical strength of the castables at medium temperature was still lower than that of CAC and reactive MgO-bonded castables. Therefore, the regulation of the hydration behavior of the HMC bond and its effect on the performance of alumina and magnesium castables need to be further investigated.

Above all, the advantages and disadvantages of the properties of the alumina-magnesia castables bonded by cement-free binders are shown in Table 2. It is shown that, in the case of ρ -Al₂O₃ and activated MgO bonded castables, the slag corrosion resistance and high-temperature performance are outstanding but the explosive spalling resistance is poor. In the case of silica sol and alumina sol bonded castables, the risk of explosive spalling of the castables is low, while the green mechanical strength at room temperature is weak. As to HMC/sol bonded castables, the properties of the green mechanical strength, the high-temperature performance, and the explosive spalling resistance are good, which skillfully integrate the inherent advantages of castables bonded by traditional hydraulic cement-free binders and sol binders, while the mid-temperature mechanical strength needs to be improved. It can be reasonably inferred that the properties of castables bonded by organic composite inorganic cement-free binders are likely to be superior to those of castables bonded by single-type cement-free binders.

Table 2. Advantages and disadvantages of the castables bonded by alumina-magnesia cement-free bonders.

Binders	Advantages	Disadvantages
ρ -Al ₂ O ₃ [14,19–22]	<ul style="list-style-type: none"> • Good slag corrosion resistance • Outstanding high-temperature performance due to no impurity components of the binder. 	<ul style="list-style-type: none"> • The castables ρ-Al₂O₃ are required a high water demanded and a longer mixing time. • The air pores are blocked by the proposed boehmite gel, resulting in the poor gas permeability of the hydration product, and high risk of explosive spalling of the castables. • Poor mechanical properties of the castables after heat treated at 300–1000 °C.
Activated MgO [39–47]	<ul style="list-style-type: none"> • Outstanding high-temperature performance • Outstanding slag corrosion resistance due to the in-suit generation of the MgAl₂O₄ spinel. 	<ul style="list-style-type: none"> • Cracking of the castables during the curing process due to the expansion of volume during the hydration of MgO and micro powders additives such as SiO₂ and Al₂O₃ are needed. • Low flowability of the castables. • A risk explosive spalling at a certain degree and drying agents are needed.
Silica sol and alumina sol [81–83,87,88,94–96]	<ul style="list-style-type: none"> • Outstanding gas permeability of the hydration product, and risk of explosive spalling of the castables due to no hydration product generation of the sol binder. • Optimization the structure of matrix and high-temperature mechanical strength of the castables resulting from the generation of nanocrystals. 	<ul style="list-style-type: none"> • Weak bonding ability of CA curing at room temperature and curing agent and heating maintenance and are required. • There is still remain in the challenges storage and transportation due to temperature sensitivity of the sol and high cost during the process of production and preparation. • Low mid-temperature mechanical strength especially at 110–800 °C.
HMC/silica sol binder [111–115]	<ul style="list-style-type: none"> • Strong binding of the binder and high green mechanical strength of the castables. • Excellent volume stability of the castables in the curing and drying process. • Good gas permeability of the hydration product, and low risk of explosive spalling of the castables. • Outstanding high-temperature performance 	<ul style="list-style-type: none"> • Poor flowability of the castables. • Low mid-temperature mechanical strength of the castables due to the decomposition of the hydration products of HMC

5. Conclusions

The application of the CAC bonded magnesia-alumina refractory castables was restricted in the environment of the secondary refining because of the low melting point phases formed. Consequently, the reduction of the content of CaO and the development of cement-free binders can effectively improve the high-temperature performance of the castables.

1. ρ -Al₂O₃ and activated MgO as traditional cement-free binders are favored of no impurities formed in the castables, so the slag corrosion resistance and thermal shock resistance of these castables are good. However, several issues are that: A large amount of water and a long mixing time are needed for the ρ -Al₂O₃; Cracking takes place of the MgO bonded constables in the curing process caused by the volume expansion of the hydration products; and a big risk of explosive spalling of these castables due to the dehydration of the hydration products. Thus, suitable additives remain to be developed.
2. The excellent explosive spalling resistance of the sol bonded castables is attributed to the binder generating no hydration product. And the high-temperature performance of the castables improved by the generation of nano- or sub-micron-sized ceramic phases in the matrix. However, the liquid phase generated by SiO₂ with other components at high temperature restricts the application. Moreover, a long curing time and low green mechanical strength are possessed by sol bonded castables. The development of novel curing agents is required.
3. The HMC is a type of organic acid magnesium binders and the HMC bonded castables have the greatest research value with good volume stability, high green mechanical strength, and excellent high-temperature performance. That's because, in suit submicron magnesia-alumina spiels are formed from the reaction between nano MgO and the Al₂O₃ in the matrix. However, a short setting time of the castables is caused by the fast hydration rate and the low mechanical strength at medium temperature caused by the decomposition of the hydration products. The hydration mechanism of HMC still needs to be further investigated, and the mechanical strength at medium temperature needs to be further enhanced, although the above problems are improved by adding MgCl₂, boric acid, SiO₂ gel.

6. Outlook

Although the application of cement-free binders poses various challenges. The development of composite binders has become the future research field of the refractories. These types of binders of hydratable magnesium carboxylate composited sol-gel, the hydratable magnesium carboxylate composited ρ -Al₂O₃, and the hydratable magnesium carboxylate composited MgO are potential. These binders show promising prospects for significantly improving the service performances of castables.

Acknowledgment

The authors acknowledge Yunqin Gao and Xing Hou, High-Temperature Ceramics Institute of Xi'an University of Architecture and Technology, for their assistance with the preparation and performance test of refractories.

Author Contributions

Conceptualization, L.S., D.D., G.X.; Investigation, L.S., J.C., and G.X.; Writing—Original Draft Preparation, L.S. and Y.F.; Writing—Review & Editing, L.S., D.D., and Y.F.; Supervision, D.D.; Project, D.D. and G.X.; Funding Acquisition, G.X.

Ethics Statement

Not applicable.

Informed Consent Statement

Not applicable for studies not involving humans.

Funding

This research was funded by the National Natural Science Foundation of China (NO. 52372034, NO. 52272027); Key R&D Project in Shaanxi Province (2023-GHZD-51, 2022GY-421).

Declaration of Competing Interest

The authors declare that they have no known competing financial interests or personal relationships that could have appeared to influence the work reported in this paper.

References

1. Huang A, Wang Y, Zou Y, Gu H, Fu L. Dynamic interaction of refractory and molten steel: Corrosion mechanism of alumina-magnesia castables. *Ceram. Int.* **2018**, *44*, 14617–14624.
2. Kumar S, Sarkar R. Alumina-spinel castable for steel ladles: An overview. *Int. J. Appl. Ceram. Technol.* **2023**, *20*, 410–423.
3. Xu S, Liu W, Liao N, Nath M, Li Y. Effect of the hydrotalcite formation on the fracture behavior and corrosion resistance of HA-bonded alumina-spinel castables. *Int. J. Appl. Ceram. Technol.* **2024**, *21*, 2993–3003.
4. Kumar S, Sarkar R. Use of alumina dispersant in alumina-spinel castable: Comparison between in situ and preformed spinels. *Int. J. Appl. Ceram. Technol.* **2024**, *21*, 1527–1542.
5. Lee WE, Vieira W, Zhang S, Ahari KG, Parr C. Castable refractory concretes. *Int. Mater. Rev.* **2001**, *46*, 3–11.
6. Sarkar R. Binders for Refractory Castables: An Overview. *InterCeram. Int. Ceram. Rev.* **2020**, *69*, 44–53.
7. Biswas S, Sarkar D. *Introduction to Refractories for Iron-and Steelmaking: Refractory for Secondary Refining of Steel*; Springer: Cham, Switzerland, 2020; pp. 329–357.
8. Matsui T, Taki N. Refractory technology of ladle. *Nippon Steel Technol. Rep.* **2020**, *415*, 52–55.
9. Halder R, Sethi S, Saravanan P, Saravanan P, Kapuri N. Effect of Submicron Reactive Alumina on the Rheological and Physico-Mechanical Properties of Microsilica Free Low Cement Castables. In Proceedings of the 41st International Committee for Study of Bauxite, Alumina & Aluminium Conference, Dubai, UAE, 5–9 November 2023; pp. 827–831.
10. Bezerra BP, Luz AP. Geopolymers: A viable binder option for ultra-low-cement and cement-free refractory castables?. *J. Eur. Ceram. Soc.* **2024**, *44*, 5241–5251.
11. Schramm T, Neubauer J, Goetz-Neunhoeffler F. Influence of silica fume addition and content on the early hydration of calcium aluminate cement-The role of soluble silicon. *Cem. Concr. Res.* **2024**, *184*, 107618.
12. Wolter CDS. Strength evolution and corrosion resistance of a cement-free Al₂O₃-castable containing a novel hydraulic binder based on α -alumina. *Refract. Worldforum* **2017**, *9*, 1–10.
13. Nevřivová L, Zemánek D. Study of the mineralogical composition of an alumina-silica binder system formed by the sol-gel method. *Materials* **2023**, *16*, 5466.
14. Zhou W, Zhang J, Zhang Z, Chen L, Ye G. Preparation and characterization of HA bonded Al₂O₃-MgO based castables with superior slag resistance for the working lining of Si-killed stainless steel ladles. *Ceram. Int.* **2022**, *48*, 18108–18115.
15. Pivinskii YE, Dyakin PV. Cement-free refractory concretes. Part 5. Cement-free refractory concretes based on hydraulic alumina binders. *Refract. Ind. Ceram.* **2020**, *61*, 374–383.
16. Li Y, Guo L, Ding D, Luo Z, Fu L, Chen L. Effect of grinding on the hydration of hydratable alumina and properties of hydratable alumina-bonded castables. *Ceram. Int.* **2021**, *47*, 6505–6512.
17. Ma W, Brown PW. Mechanisms of reaction of hydratable aluminas. *J. Am. Ceram. Soc.* **1999**, *82*, 453–456.
18. Oliveira IR, Pandolfelli VC. Castable matrix, additives and their role on hydraulic binder hydration. *Ceram. Int.* **2009**, *35*, 1453–1460.
19. Salomao R, Ismael MR, Pandolfelli VC. Hydraulic binders for refractory castables: Mixing, curing and drying. *Ceram. Forum Int.* **2007**, *84*, 103–108.
20. Fábio A, Innocentini MDM, Miranda MFS, Valenzuela FAO, Pandolfelli VC. Drying behavior of hydratable alumina-bonded refractory castables. *J. Eur. Ceram. Soc.* **2004**, *24*, 797–802.
21. Nana X. *Hydration and Dehydration Mechanism of Hydratable Alumina and Its Performance in Combination with Al₂O₃-MgO Castables*; Wuhan University of Science and Technology: Wuhan, China, 2019; pp. 51–52.
22. Souza ADV, Arruda CC, Fernandes L, Antunes MLP, Kiyohara PK, Salomão R. Characterization of aluminum hydroxide (Al(OH)₃) for its use as a porogenic agent in castable ceramics. *J. Europ. Ceram. Soc.* **2015**, *35*, 803–812.
23. Salomão R, Kawamura MA, Souza ADV, Sakihama J. Hydratable alumina-bonded suspensions: evolution of microstructure and physical properties during first heating. *InterCeram. Int. Ceram. Rev.* **2017**, *66*, 28–37.
24. Ye G, Troczynski T. Hydration of hydratable alumina in the presence of various forms of MgO. *Ceram. Int.* **2006**, *32*, 257–262.
25. Xu N, Li Y, Fang S, Li S, Wang H, Xiang R, et al. Hydration behavior and microstructural evolution of hydratable alumina with different particle size in alumina-spinel castables. *J. Ceram. Soc. Jpn.* **2019**, *127*, 199–206.
26. Li Y, Zhang H, Guo L, Zhang P, Wang G, Zhai P, et al. Effect of hydromagnesite on the hydration of hydratable alumina and properties of corundum-based castables. *Ceram. Int.* **2022**, *48*, 36383–36392.
27. Xu N, Li Y, Li S, Wang H, Xiang R, Ouyang S. Controlled morphologies and hydration process of hydratable alumina by using citric acid. *J. Aust. Ceram. Soc.* **2020**, *56*, 1427–1433.

28. Xu N, Li Y, Li S, Wang H, Xiang R, Ouyang S. Hydration mechanism and sintering characteristics of hydratable alumina with microsilica addition. *Ceram. Int.* **2019**, *45*, 13780–13786.
29. Rangdal P, Patil SB, Hiremath P. Study on Drying Behavior of Hydratable Alumina-bonded High-Alumina Castables by Addition of Different Organic Fibers. *J. Inst. Eng.* **2024**, *105*, 183–189.
30. Wang H, Wang Z, Feng H, Cao Y, Liu J, Xu Y. Effect of H₂O₂ Addition on anti-explosion performance of ρ -Al₂O₃ bonded corundum castables. *China Refract.* **2023**, *32*, 14–19.
31. Salomão R, Pandolfelli VC. Dryout temperature-vapor pressure profile of polymeric fiber containing refractory castables. *Ceram. Int.* **2013**, *39*, 7217–7222.
32. Salomão R, Pandolfelli VC. Anti-spalling fibers for refractory castables: A potential application for recycling drinking straws. *Ceram. Int.* **2020**, *46*, 14262–14268.
33. Salomão R, Cardoso FA, Bittencourt LRM. Effect of polymeric fibers on refractory castable permeability. *Am. Ceram. Soc. Bull.* **2003**, *82*, 51–56.
34. Salomão R, Isaac CS, Pandolfelli VC. Natural fibers as drying additives for refractory castables. *Am. Ceram. Soc. Bull.* **2004**, *83*, 9201–9205.
35. Wöhrmeyer C, Auvray JM, Zetterstrom C. Dry out of dense refractory castables dry out of dense refractory castables via use of permeability enhancing active compound. In Proceedings of the 59th International Colloquium on Refractorie, Aachen, Germany, 28–29 September 2016; pp. 40–44.
36. Parr C, Alt C, Auvray JM, Fryda H, Wöhrmeyer C. Quick drying castables quick drying castables based upon 80% alumina cement. In Proceedings of the Symposium on refractories, Louis, MO, USA, 14–18 February 2010; pp. 1–11.
37. Ismael MR, Anjos RD, Salomão R, Pandolfelli VC. Colloidal silica as a nanostructured binder for refractory castables. *Refract. Appl. News* **2006**, *11*, 16–20.
38. Pinto VS, Fini DS, Miguel VC, Pandolfelli VC, Moreira MH, Venâncio T, et al. Fast drying of high-alumina MgO-bonded refractory castables. *Ceram. Int.* **2020**, *46*, 11137–11148.
39. Winnefeld F, Epifania E, Montagnaro F, Gartner EM. Further studies of the hydration of MgO-hydromagnesite blends. *Cem. Concr. Res.* **2019**, *126*, 105912.
40. Wang Z, Park S, Khalid H, Lee HK. Hydration properties of alkali-activated fly ash/slag binders modified by MgO with different reactivity. *J. Build. Eng.* **2021**, *44*, 103252.
41. Sako EY, Braulio MAL, Pandolfelli VC. Advanced understanding on in situ spinel formation and corrosion performance of spinel-containing refractory castables. In Proceedings of the Unified International Technical Conference on Refractories, Victoria, Australia, 11 September 2013; pp. 597–601.
42. Li Y, Li G, Liu G. A post-mortem analysis of the used gel-bonded Al₂O₃–MgAl₂O₄ castables in an industrial steelmaking ladle. *Int. J. Appl. Ceram. Technol.* **2023**, *20*, 1978–1989.
43. Mo L, Deng M, Tang M. Effects of calcination condition on expansion property of MgO-type expansive agent used in cement-based materials. *Cem. Concr. Res.* **2010**, *40*, 437–446.
44. Rocha SD, Mansur MB, Ciminelli VS. Kinetics and mechanistic analysis of caustic magnesia hydration. *J. Chem. Technol. Biotechnol.* **2004**, *79*, 816–821.
45. Souza TM, Braulio MAL, Luz AP, Bonadia P, Pandolfelli VC. Systemic analysis of MgO hydration effects on alumina-magnesia refractory castables. *Ceram. Int.* **2012**, *38*, 3969–3976.
46. Wang Y, Wang Z, Wang X, Liu H, Ma Y, Jiang P. Progress in the research of anti-burst cracking of refractory castables. *J. Silic.* **2022**, *50*, 1762–1774.
47. Wang JA, Novaro O, Bokhimi X, López T, Gómez R, Navarrete J, et al. Characterizations of the thermal decomposition of brucite prepared by sol-gel technique for synthesis of nanocrystalline MgO. *Mater. Lett.* **1998**, *35*, 317–323.
48. Luz AP, Consoni LB, Pagliosa C, Aneziris CG, Pandolfelli VC. MgO fumes as a potential binder for in situ spinel containing refractory castables. *Ceram. Int.* **2018**, *44*, 15453–15463.
49. Warmuz K, Madej D. Effect of the particle size on the reactivity of MgO–Al₂O₃ hydrating mixtures: A long-term kinetic investigation of hydrotalcite synthesis. *Appl. Clay Sci.* **2021**, *211*, 106196.
50. Dos Santos T, dos Santos J, Luz AP, Pagliosa C, Pandolfelli VC. Kinetic control of MgO hydration in refractory castables by using carboxylic acids. *J. Eur. Ceram. Soc.* **2018**, *38*, 2152–2163.
51. Santos T, Luz AP, Pagliosa C, Pandolfelli VC, Rigaud M. Mg(OH)₂ nucleation and growth parameters applicable for the development of MgO-based refractory castables. *J. Am. Ceram. Soc.* **2016**, *99*, 461–469.
52. Dung NT, Unluer C. Influence of nucleation seeding on the performance of carbonated MgO formulations. *Cem. Concr. Compos.* **2017**, *83*, 1–9.
53. Filippou D, Katiforis N, Papassiopi N, Adam K. On the kinetics of magnesia hydration in magnesium acetate solutions. *J. Chem. Technol. Biotechnol.* **1999**, *74*, 322–328.
54. Souza TM, Luz AP, Braulio MAL, Pagliosa C, Pandolfelli VC, Rigaud M. Acetic acid role on magnesia hydration for cement-free refractory castables. *J. Am. Ceram. Soc.* **2014**, *97*, 1233–1241.
55. Amaral LF, Oliveira IR, Salomão R, Frollini E, Pandolfelli VC. Temperature and common-ion effect on magnesium oxide

- (MgO) hydration. *Ceram. Int.* **2010**, *36*, 1047–1054.
56. Chen S, Chen G, Cheng J, Tian F. Effect of additives on the hydration resistance of materials synthesized from the magnesia-calcia system. *J. Am. Ceram. Soc.* **2000**, *83*, 1810–1812.
 57. Wang H, Liang S, Zhou X, Hou P, Cheng X. Regulating hydration and microstructure development of reactive MgO cement by citric acids. *Cement. Concrete. Comp.* **2025**, *155*, 105832.
 58. Chen J, Huang L, Dong L, Zhang H, Huang Z, Li F, et al. Hydration behavior of MgO surface: A first-principles study. *Appl. Surf. Sci.* **2023**, *611*, 155441.
 59. Souza TM, Luz AP, Santos T, Gimenes DC, Miglioli MM, Correa AM, et al. Phosphate chemical binder as an anti-hydration additive for Al₂O₃-MgO refractory castables. *Ceram. Int.* **2014**, *40*, 1503–1512.
 60. Szczerba J, Prorok R, Czapka Z, Madej D, Niek E, Jastrzbska I. Influence of microsilica on mechanical properties of basic castables. In Proceedings of the Unified International Technical Conference on Refractories, Hoboken, NJ, USA, 7 March 2014; pp. 1013–1018.
 61. Taj K, Akturk B, Ulukaya S. Influence of carbonation curing and nano-silica incorporation on compressive strength and microstructural development of binary RMC-based systems. *J. Build. Eng.* **2023**, *66*, 105856.
 62. Zhang Y. *Generation of Hydrated Magnesium Silicate in Magnesium Castables and Its Effect on Material Properties*; Wuhan University of Science and Technology: Wuhan, China, 2018; pp. 25–29.
 63. Bernard E, Lothenbach B, Rentsch D, Pochard I, Dauzères A. Formation of magnesium silicate hydrates (M-S-H). *Phys. Chem. Earth* **2017**, *99*, 142–157.
 64. Li Y, Liao N, Liu W, Zhang S, Xu Y, Tie S, et al. Preparation of low-silica magnesium castables based on the structure memory property of hydrated magnesium silicate. *J. Silic.* **2023**, *51*, 649–657.
 65. Zhang Y, Li Y, Xu Y, Sang S, Jin S. Enhanced formation of magnesium silica hydrates (M-S-H) using sodium metasilicate and caustic magnesia in magnesia castables. *Ceram. Int.* **2017**, *43*, 9110–9116.
 66. Peng H, Luo M, Myhre B. New additive packages for self-flowing high-alumina and MgO based refractory castables. In Proceedings of the Asociación Latinoamericana de Fabricantes de Refractorios, Cancun, Mexico, 13–16 October 2012; pp. 1–13.
 67. Peng H, Myhre B. Microsilica-gel bonded self-flowing MgO castables using a new additive package. In Proceedings of the Unified International Technical Conference on Refractories, Kolkata, India, 15–18 January 2014; pp. 1–7.
 68. Santos TD, Krol LF, Luz AP. Evaluation of a microsilica-based additives in Al₂O₃-MgO refractory castables. *Refract. Worldforum* **2019**, *9*, 11.
 69. Peng H, Myhre B. Crack of MgO castable: a challenge of the past? In Proceedings of the Unified International Technical Conference on Refractories, Aachen, Germany, 16–17 September 2020; pp. 56–60.
 70. Zhang S, Liao N, Li Y, Chatterjee A, Zhang Y, Sang S. M-S-H formation in MgO-SiO₂ slurries via wet milling for magnesia based castables. *Ceram. Int.* **2021**, *47*, 10880–10886.
 71. Fini DS, Miguel VC, Pinto VS. Aluminum lactate role in improving hydration and drying behavior of MgO-bonded refractory castables. *Ceram. Int.* **2020**, *46*, 17093–17102.
 72. Yeh S, Lin W, Liu P, Chen H. Ways to overcome the preheating explosion of alumina spinel-forming castable. In Proceedings of the Unified International Technical Conference on Refractories, Vienna, Austria, 15–18 September 2015; pp. 1–4.
 73. Consonni LB, Da Luz AP, Pandolfelli VC. Evaluation of the combined addition of aluminum lactate and calcium carbonate to alumina-based castables. *Cerâmica* **2021**, *67*, 196–202.
 74. Salomão R, Martinatti IS, Fernandes L, Sundblom A, Greenwood P, Tiba PRT. Novel silanized colloidal silica-MgO self-flowing dispersions with improved hydroxylation resistance. *J. Eur. Ceram. Soc.* **2023**, *43*, 5691–5705.
 75. Warmuz K, Madej D. Synthesis and evaluation of Mg-Al hydrotalcite formation and its influence on the microstructural evolution of spinel-forming refractory castables under intermediate temperatures. *J. Eur. Ceram. Soc.* **2022**, *42*, 2545–2555.
 76. Li Y, Xu S, Liao N, Nath M, Chatterjee A, Tie, S. The in-situ formation of Mg-Al hydrotalcite and its effect on the properties of MgO-bonded alumina castables. *Constr. Build. Mater.* **2023**, *404*, 133242.
 77. Sato T, Ikoma S, Ozawa F. Thermal decomposition of aluminium hydroxycarboxylates-lactate, citrate and tartrate. *J. Chem. Tech. Biotech.* **1983**, *33*, 415–420.
 78. Hashishin T, Joyama A, Kaneko Y. Effect of aluminum lactate powder in the production of mullite porous bodies. *J. Ceram. Soc. Jpn.* **2010**, *106*, 127–130.
 79. Pivinskii YE. Cement-free refractory concretes. Part 4. Refractory concretes based on silica sol binders. *Refract. Ind. Ceram.* **2020**, *61*, 150–158.
 80. Wen L, Xu J, Yang Q, Zhang F, Li F, Zhang L. Gelation process of nanosilica sol and its mechanism: Molecular dynamics simulation. *Chem. Eng. Sci.* **2020**, *216*, 115538.
 81. Singh AK. *Study on the Effect of Different Sols on High Alumina Castable Refractory*; Ceramic Engineering Department, National Institute of Technology: Rourkela, India, 2017; pp. 75–84.
 82. Lang C, Delmotte C, Vandeneede V, Thiesen M, Ibarra L, Dannert C. Investigation of the milling route for the development of colloidal suspensions to be used as a binder in refractory castables. *Open Ceram.* **2023**, *15*, 100394.

83. Nouri-Khezrabad M, Braulio MAL, Pandolfelli VC, Golestani-Fard F, Rezaie HR. Nano-bonded refractory castables. *Ceram. Int.* **2013**, *39*, 3479–3497.
84. Dos Anjos RD, Ismael MR, Oliveira IR, Pandolfelli VC. Workability and setting parameters evaluation of colloidal silica bonded refractory suspensions. *Ceram. Int.* **2008**, *34*, 165–171.
85. Chatterji S. Colloid electrochemistry of saturated cement paste and some properties of cement based materials. *Adv. Cem. Based Mater.* **1998**, *7*, 102–108.
86. Sarathchandran C, Renjith PK, Sekkar V. *Engineering of Natural Polymeric Gels and Aerogels for Multifunctional Applications: Silica Aerogels: Synthesis, Properties, and Applications*; Elsevier: Amsterdam, The Netherlands, 2024; pp. 313–342.
87. Hossain SS, Roy PK. Waste rice husk ash derived sol: A potential binder in high alumina refractory castables as a replacement of hydraulic binder. *J. Alloys Compd.* **2020**, *817*, 152806.
88. Wang Y, Chen P, Zhu B. Research status and prospect of silicon-aluminium sol as a binder for refractory castables. *J. Silic.* **2017**, *45*, 422–432.
89. Milani SS, Kakroudi MG, Vafa NP. Properties of alumina sol prepared via inorganic route. *Ceram. Int.* **2020**, *46*, 9492–9497
90. Wang Y, Wang M, Hu C, Jia Y. Preparation and characterisation of alumina sol. *Tianjin Chem. Ind.* **2020**, *34*, 19–22.
91. Iijima S, Yumura T, Liu Z. One-dimensional nanowires of pseudoboehmite (aluminum oxyhydroxide γ -AlOOH). *Proc. Natl. Acad. Sci. USA* **2016**, *113*, 11759–11764.
92. Singh AK, Sarkar R. Synthesis and characterization of alumina sol and its use as binder in no cement high-alumina refractory castables. *Int. J. Appl. Ceram. Technol.* **2015**, *12*, 169.
93. Shapovalova OE, Drozdov AS, Bryushkova EA, Morozov MI, Vinogradov VV. Room-temperature fabrication of magnetite-boehmite sol-gel composites for heavy metal ions removal. *Arab. J. Chem.* **2020**, *13*, 1933–1944.
94. Mohammadi M, Khodamorady M, Tahmasbi B, Bahrami K, Ghorbani-Choghmarani A. Boehmite nanoparticles as versatile support for organic-inorganic hybrid materials: Synthesis, functionalization, and applications in eco-friendly catalysis. *J. Ind. Eng. Chem.* **2021**, *97*, 1–78.
95. Majerová J, Sklenářová D, Nevřivová L. The effect of the type of gelling agent on the speed of gelation of sol-gels. *Solid State Phenom.* **2023**, *351*, 47–52.
96. Braulio M, Tontrup C, Medeiros J. Colloidal alumina as a novel castable bonding system. *Refract. Worldforum* **2011**, *3*, 135–141.
97. Huang Y, Yang N, Zhang Y, Hou J, Gao Y, Tian L, et al. The gelling behavior of gellan in the presence of different sodium salts. *Int. J. Biol. Macromol.* **2021**, *193*, 768–777.
98. Lee GW, Kim SH, Lee DY, Lee K-Y, Chun B, Jung HW. Effect of solution pH on the microstructural and rheological properties in boehmite suspensions. *Korea-Aust. Rheol. J.* **2023**, *35*, 1–10.
99. Dronova M, Lécolier E, Barré L, Michot LJ. Phase diagram, structure and rheology of boehmite dispersions: Role of electrostatic interactions. *Colloids Surf.* **2021**, *631*, 127564.
100. Grządka E, Matusiak J. The effect of ionic and non-ionic surfactants and pH on the stability, adsorption and electrokinetic properties of the alginic acid/alumina system. *Carbohydr. Polym.* **2017**, *175*, 192–198.
101. Prabhakaran K, Ananthakumar S, Pavithran C. Preparation of extrudable alumina paste by coagulation of electrosterically stabilized aqueous slurries. *J. Eur. Ceram. Soc.* **2002**, *22*, 153–158.
102. Magliano MVM, Prestes E, Medeiros J, Veiga J, Pandolfelli VC. Colloidal silica selection for nanobonded refractory castables. *Refract. Appl. News* **2010**, *15*, 14–17.
103. Parr C, Wohrmeyer C. The advantages of calcium aluminate cement as a castable bonding system. In Proceedings of the Lafarge Aluminates Paris, Paris, France, 2006; pp.1–20.
104. Cichocki M, Angelkort J, Fröse N, Higgins S, Knoll M, Mix M. The Binding of non-cement refractory castables using the technology of in-situ sol-gel formation. *Intocast* **2023**, *1*, 1–3.
105. Qiu W, Ruan G, Zhang Z. Properties of silica sol bonded corundum-spinel castables for steel ladles. *Int. J. Appl. Ceram. Technol.* **2018**, *15*, 1182–1189.
106. Neese J, Kesselheim B, Rollmann S. Hybrid technology-advance for sol-gel bonded refractory concrete. *Refract. Worldforum* **2019**, *11*, 11037.
107. Raj SJS, Vidyavathy SM. Effects of mullite gel on the properties of alumina castables. *J. Ceram. Process. Res.* **2021**, *22*, 636–641.
108. Singh AK, Sarkar R. High alumina castables: A comparison among various sol-gel bonding systems. *J. Aust. Ceram. Soc.* **2017**, *53*, 553–567.
109. Wang J. *Preparation of Spinel Precursor Sol and Its Effect on the Properties of Alumina-Based Castables*; Sinosteel Group Luoyang Refractories Research Institute Limited: Luoyang, China, 2023; pp. 17–74
110. Chen J, Xiao G, Ding D, Zang Y, Lei C, Luo J, et al. Thermal shock resistance properties of refractory castables bonded with a CaO-free binder. *Ceram. Int.* **2021**, *47*, 4238–4248.
111. Xiao G, Chen J, Ding D, Lei C, Zang Y, Chong X, et al. Enhanced thermal shock resistance of hydratable magnesium

- carboxylate bonded castables via in-situ formation of micro-sized spinel. *Ceram. Int.* **2021**, *47*, 29423–29434.
112. Chen J, Xiao G, Ding D, Zhang S, Lei C, Zang Y, et al. Mechanical properties of refractory castables bonded with hydratable magnesium carboxylate-boric acid. *Ceram. Int.* **2021**, *47*, 21221–21230.
113. Zheng W, Liu X, Song X. Metallurgical behaviour of boron in the steelmaking process and its effect on the mechanical properties of steel plates. *J. Liaoning Univ. Sci. Technol.* **2019**, *42*, 406–409.
114. Chen J, Xiao G, Ding D, Sun L, Zang Y, Yin C, et al. Improving the mechanical property of the castables bonded with hydratable magnesium carboxylate by incorporating MgO fumes. *Int. J. Appl. Ceram. Technol.* **2024**, *21*, 2321–2331.
115. Sun L, Ding D, Xiao G, Li Y, Kang J, Lei C, et al. Mechanical properties and gas permeability of silica-gel modified hydratable magnesium carboxylate bonded refractory castables in drying process. *Ceram. Int.* **2024**, *50*, 13356–13365.